Impacts of gravitational-wave background from supermassive black hole binaries on the detection of compact binaries by LISA*

Fan Huang (黄帆)[1,2†] Yan-Chen Bi (毕研晨)[1,2‡] Zhoujian Cao (曹周键)[3,4§] Qing-Guo Huang (黄庆国)[1,2,4¶]

[1]CAS Key Laboratory of Theoretical Physics, Institute of Theoretical Physics, Chinese Academy of Sciences, Beijing 100190, China
[2]School of Physical Sciences, University of Chinese Academy of Sciences, Beijing 100049, China
[3]Institute of Applied Mathematics, Academy of Mathematics and Systems Science, Chinese Academy of Sciences, Beijing 100190, China
[4]School of Fundamental Physics and Mathematical Sciences, Hangzhou Institute for Advanced Study, UCAS, Hangzhou 310024, China

Abstract: In the frequency band of the Laser Interferometer Space Antenna (LISA), extensive research has been conducted on the impact of foreground confusion noise generated by galactic binaries within the Milky Way Galaxy. Additionally, recent evidence of a stochastic signal, announced by the NANOGrav, EPTA, PPTA, CPTA, and InPTA, indicates that the stochastic gravitational-wave background (SGWB) generated by supermassive black hole binaries (SMBHBs) can contribute strong background noise within the LISA band. Given the presence of such strong noise, it is expected to have significant impacts on LISA's scientific missions. In this study, we investigate the impacts of the SGWB generated by SMBHBs on the detection of individual massive black hole binaries, verified galactic binaries, and extreme mass ratio inspirals in the context of LISA. We find it essential to resolve and eliminate the excess noise from the SGWB to guarantee the success of LISA's missions.

Keywords: gravitational-wave background, supermassive black hole binaries, LISA

DOI: 10.1088/1674-1137/ad34c2

I. INTRODUCTION

The Laser Interferometer Space Antenna (LISA) is a space-borne gravitational wave (GW) detector operating in the frequency band of approximately $10^{-4} \sim 10^{-1}$ Hz [1−3]. This low-frequency band is abundant in a variety of GW sources that will enable us to observe the universe in a new and unique way, yielding insights in a wide range of topics in astrophysics and cosmology.

LISA has proposed a multitude of scientific objectives (SOs) associated with the necessary observation requirements for their fulfillment. These observation requirements are, in turn, related to mission requirements (MRs) pertaining to noise performance, mission duration, *etc.*, which require the calculation of the signal-to-noise-ratio (SNR) for assessment [2]. Different noise performance levels can lead to significant variations in the SNR for a specific GW source. Meanwhile, the detectability and parameter measurement accuracy of this source will also be affected by the noise.

According to the 2017 LISA design [2], the strain sensitivity curves of LISA are composed of the combination of predicted Michelson-equivalent sensitivity and stochastic GW background (SGWB) noise. In previous papers, the foreground noise around 10^{-3} Hz due to a galactic binary [4−6] and the SGWB above 10^{-3} Hz from stellar origin black holes (SOBHs) [7] were discussed. Moreover, recent evidence of a stochastic signal consistent with the SGWB in the spectrum from $10^{-9} \sim 10^{-1}$ Hz, announced by the North American Nanohertz Observatory for Gravitational Waves (NANOGrav) [8−10], the European Pulsar Timing Array (EPTA) in collaboration with the Indian Pulsar Timing Array (InPTA) [11, 12], the Parkes Pulsar Timing Array (PPTA) [13, 14], and the Chinese Pulsar Timing Array (CPTA) [15, 16], indicates that the SGWB due to supermassive black hole binaries (SMBHBs) can significantly contribute to background noise in LISA frequency band [17−21], introducing potential challenges to the LISA mission. However, this influence has not yet been extensively investigated.

In this study, we utilize the up-to-date SGWB data from the SMBHB indicated by the NANOGrav 15-year dataset to investigate its impacts on the LISA mission. Because the majority of individual LISA sources will be

Received 21 February 2024; Accepted 15 March 2024; Published online 16 March 2024
* Supported by the NSFC (12250010, 11991052) and Key Research Program of Frontier Sciences, CAS, (ZDBS-LY-7009)
† E-mail: huangfan@itp.ac.cn
‡ E-mail: biyanchen@itp.ac.cn
§ E-mail: zjcao@amt.ac.cn
¶ E-mail: huangqg@itp.ac.cn

binary systems covering a broad range of masses [2, 3], we address the impacts of the SGWB generated by SMBHBs on the detection of compact binaries in the LISA mission. More specifically, we examine the effect on the detection of individual massive black hole binaries (MBHBs), verified galactic binaries (VGBs), and extreme mass ratio inspirals (EMRIs).

II. ENLIGHTENMENT FROM THE PTA RESULTS

SMBHBs are the most promising sources to explain the origin of recent PTA results. It is important to note that the astrophysically motivated models of SMBHB populations are able to reproduce the observed low-frequency GW spectrum in an elegant manner [17, 19]. We adopt these astrophysically motivated models [19, 22] and inspiral-merger-ringdown waveforms [23, 24] to obtain the full spectrum of SMBHBs. Then, the present-day energy density of the SGWB of SMBHBs $\Omega_{\rm GW}(f)$ is given by [25]

$$\Omega_{\rm GW}(f)=\frac{8\pi G f}{3H_0^2c^2}\int {\rm d}z{\rm d}\mathcal{M}\frac{{\rm d}^2n}{{\rm d}z{\rm d}\mathcal{M}}\frac{{\rm d}E_{\rm GW}}{{\rm d}f_r}, \tag{1}$$

where $H_0=67.4\ {\rm km\ sec^{-1}\ Mpc^{-1}}$ [26] is the Hubble constant, and $f_r=(1+z)f$ is the source-frame GW frequency. Here, $\mathcal{M}=Mq^{3/5}/(1+q)^{1/5}$ is the chirp mass of the SMBHB, where M is the primary mass, and q is the mass ratio of the black hole. Moreover, ${\rm d}^2n/{\rm d}z{\rm d}\mathcal{M}$ refers to the SMBHB population. The relevant ranges in the integrals are $0\le z\le 5$ and $10^5M_\odot\le\mathcal{M}\le 10^{11}M_\odot$.

The SMBHB population of this model can be obtained from the galaxy population as

$$\frac{{\rm d}^3n_G}{{\rm d}z'{\rm d}M_G{\rm d}q_G}=\frac{\Phi(M_G,z)}{M_G\ln 10}\frac{\mathcal{F}(M_G,z,q_G)}{\tau(M_G,z,q_G)}\frac{{\rm d}t_r}{{\rm d}z}, \tag{2}$$

where z denotes the redshift of the galaxy pair, z' is the redshift at galaxy pair merging, and they are connected by the merger timescale of the galaxy pair $\tau(M_G,z,q_G)$. Moreover, there is a correlation between the mass of a galaxy and the mass of the supermassive black hole (SMBH) at its center, known as the SMBH-Host relation [22, 27], which translates the galaxy mass M_G to the black hole mass M. The Bayesian inference method is employed to obtain the posterior distributions of the parameters that are yet to be determined in the model [19]. The posterior can be presented as

$$p(\Theta|d)\propto\mathcal{L}(d|\Theta)p(\Theta), \tag{3}$$

where $p(\Theta)$ are the priors on the population parameters obtained from astrophysical obervation [19, 22], and the likelihood $\mathcal{L}(d|\Theta)$ is computed from the NANOGrav 15-yr free-spectrum.

III. SENSITIVITY OF LISA

Here, we adopt the analytic-fit sensitivity curve $S_a(f)$ for the Michelson-style LISA data channel given by [5]:

$$S_a(f)=\frac{10}{3L^2}\left(P_{\rm OMS}(f)+2(1+\cos^2(f/f_*))\frac{P_{\rm acc}(f)}{(2\pi f)^4}\right)\times\left(1+\frac{6}{10}\left(\frac{f}{f_*}\right)^2\right), \tag{4}$$

where the transfer frequency $f_*=19.09$ mHz, and arm length $L=2.5\times10^6$ km. In addition to the instrument noise, the galactic confusion noise, also called the stochastic foreground, generated by unresolved galactic binaries will contribute extra noise $S_c(f)$ to sensitivity; therefore, LISA's effective strain sensitivity curve $S_n(f)$ becomes the sum of $S_a(f)$ and $S_c(f)$ [2, 4–6]. The detailed expressions for single-link metrology noise $P_{\rm OMS}(f)$, single test mass acceleration noise $P_{\rm acc}(f)$, and galactic confusion noise $S_c(f)$ are given in [5]. Such additives of strain sensitivity indicate that we may calculate the impacts of the SGWB by summing its corresponding strain sensitivity $S_{\rm GW}(f)$ to $S_n(f)$.

Following the methods proposed by [4, 5], we define the noise strain sensitivity due to the SGWB as

$$S_{\rm GW}(f)=\frac{3H_0^2}{2\pi^2}\frac{\Omega_{\rm GW}(f)}{f^3}, \tag{5}$$

which can be added to the strain sensitivity of LISA with galactic confusion noise $S_n(f)$ to obtain an effective strain sensitivity $S_{\rm eff}(f)=S_n(f)+S_{\rm GW}(f)$ [2, 4–6], and then the SNR affected by the presence of the GW background can be written as

$${\rm SNR}=2\left(\int {\rm d}f\frac{|\tilde{h}(f)|^2}{S_{\rm eff}(f)}\right)^{1/2}, \tag{6}$$

where $\tilde{h}(f)$ is the frequency domain representation of the time-domain waveform $h(t)$, which encodes important information on the intrinsic parameters of the GW source.

In Fig. 1, we present the effective characteristic strain $S_{\rm eff}(f)$ influenced by the SGWB originating from SMBHBs together with the specific GW signals of VGBs and an illustrative example of EMRIs. The effective characteristic strain, which represents the cumulative impact of all SMBHBs, is depicted as the burlywood-colored region in Fig. 1. Notably, within the frequency range below several 10^{-2} Hz, it experiences a dramatic increase, partially obscuring specific signals associated with VGBs

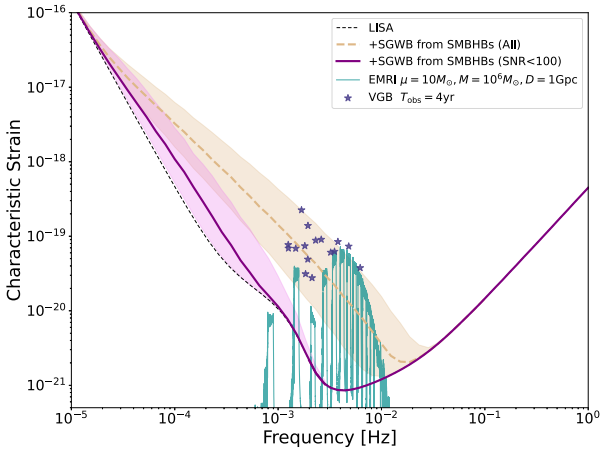

Fig. 1. (color online) Expected effective characteristic strain $S_{\rm eff}(f)$ in the frequency range $[10^{-5},1]$ Hz. The burlywood line represents the effective characteristic strain derived from the SGWB of all SMBHBs, whereas the purple line illustrates the effective characteristic strain obtained from the SGWB of SMBHBs after excluding those with SNR≥100. The shaded regions in both cases indicate the 90% credible intervals. Additionally, we depict the expected characteristic strain curves of LISA as black dashed lines. The dark cyan line corresponds to the characteristic strain produced by an illustrative EMRI signal [33], whereas the star marker represents VGB signals [34, 35].

and EMRIs. It is believed that GW signals from SMBHBs with SNRs equal to or greater than $O(100)$ (we set 100 as the criteria to be on the safe side) can be resolved and eliminated from the SGWB, as indicated in [2, 28]. Our approach involves using $S_{\rm eff}(f)$, which accounts for contributions from all SMBHBs, as a baseline. We iteratively eliminate the contributions from SMBHB events with SNR ≥ 100 and derive a new effective characteristic strain. This iterative process continues until the effective characteristic strain reaches convergence.

Although the vast majority of SMBHB signals in LISA's band with SNRs above $8\sim12$ are individually resolvable [2, 3, 29], recent studies on unresolved SGWBs from compact binary mergers in the frequency band of next-generation ground-based GW observatories [30−32] suggest that the residual GW background $\Omega_{\rm residual}$ might be still considerable after subtraction, where $\Omega_{\rm residual}$ is the combination of the unresolved background $\Omega_{\rm unres}$ and error background $\Omega_{\rm error}$ due to the uncertainty in parameter estimation during the subtraction procedure. Because $\Omega_{\rm residual} = \Omega_{\rm unres} + \Omega_{\rm error}$ of a GW observatory depends on its SNR threshold for confusion noise elimination, the lower the SNR threshold, the lower the $\Omega_{\rm unres}$ but higher the $\Omega_{\rm error}$ [30]. We adopt the threshold SNR = 100 to reduce $\Omega_{\rm error}$ to a negligible level, given that the error background from compact binary mergers in LISA's band still requires study.

As a result, the shift in the characteristic strain, represented by the purple-colored region in Fig. 1, becomes reduced compared to that in the non-eliminated scenario. Furthermore, the frequency band influenced by the SGWB shifts from several 10^{-2} Hz to a few 10^{-3} Hz, moving away from LISA's most sensitive range.

Given that the MRs of LISA set the requirement of a minimum SNR level for specific detectable sources, we further discuss the impact of the SGWB on LISA's detection in terms of variations in the SNR in the subsequent sections.

IV. DETECTABILITY OF MBHBs

MBHBs are categorized by two types, intermediate mass black holes binaries (IMBHBs) with an intermediate mass range between several hundreds and $10^5M_\odot$ for each black holes and SMBHBs with masses above $10^5M_\odot$. Tracing the origin, growth, and merger history of MBHs across cosmic ages is a vital SO of LISA.

The origin of MBHs lurking at the centers of galaxies as power source of active galactic nuclei is an on-going topic. Some studies predict the mass range of their seeds to be around $10^3M_\odot$ to a few $10^5M_\odot$ within the formation redshift $10\sim15$ [36]. After accretion episodes and repeated merging in the period of cosmic structure clustering, these seeds can grow up to $10^8M_\odot$ and greater [37]. During the growth of seeds, accretion and mergers imprint different information on their spins. To measure the dimensionless spins and misalignment of spins with the orbital angular momentum with low absolute error, the accumulated SNR (from the inspiral phase up to merger) is required to reach a certain level.

When studying the growth mechanism of MBHs from the epoch of the earliest quasars, an accumulated SNR of at least ~ 200 is required to ensure the accurate measurement of parameters. This SNR requirement is also needed to test the propagation of GWs in LISA's science investigations (SIs) [2].

In the absence of an SGWB, the expected minimum observation rate of several MBHBs per year would fulfill the requirements of SO2, assuming a conservative population model [38].

In Fig. 2, we present contour plots of an SNR with a value of SNR = 200 using the waveform model derived from Refs. [23, 24]. These plots depict the SNR values for GW signals emitted by MBHBs, both in the presence and absence of the SGWB generated by SMBHBs. The plots are presented in the plane with the source-frame total mass (M) and redshift (z) of the sources. Without loss of generality, we assume a mass ratio of 0.2 for the binary systems. This choice corresponds to the parameterization used in LISA's Sensitivity Curve SI 2.1, which is designed for the search for seed black holes at cosmic dawn [2].

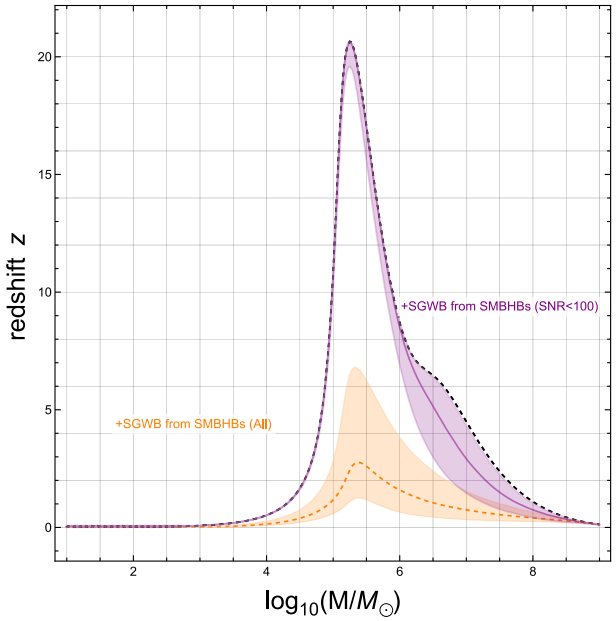

Fig. 2. (color online) LISA's SNR=200 curves for the GW signals of MBHBs with and without the presence of the SGWB generated by SMBHBs, in the plane of total source-frame with mass M and redshift z. The mass ratio of binaries q is 0.2. The black dashed line is the curve without consideration of the SGWB from SMBHBs. The orange line shows the curve under the effect of the SGWB from all SMBHBs combined, and the purple line is the curve under the effect of the SGWB from SMBHBs where all the signals with SNR≥100 are resolved and eliminated. The shaded regions indicate the corresponding 90% credible intervals.

Our analysis reveals a significant reduction in the detectable redshift of GW signals generated by MBHBs with an SNR of 200 in the mass range $10^4 \sim 10^8 M_\odot$. This reduction occurs when the SGWB from SMBHBs cannot be resolved and eliminated during the observation period. Given that the goals of LISA SI 2.2 involve the detection of sources at redshift $z < 3$ with masses ranging from 10^5 to $10^6 M_\odot$ and an accumulated SNR of at least approximately 200, the presence of the SGWB has a substantial impact on this investigation.

However, should we succeed in resolving and eliminating GW signals with SNR values greater than or equal to 100, the impact on the detection of MBHBs in the LISA mission will be significantly reduced. Consequently, the objectives of SI 2.2 will be slightly affected for MBHBs with masses exceeding $10^6\ M_\odot$.

V. DETECTABILITIES OF VGBs AND EMRIs

Because there are large numbers of compact binaries in the Milky Way Galaxy that emit continuous and nearly monochromatic electromagnetic (EM) signals, parts of these binaries are already verified by observations other than GW detection. For VGBs emitting GW signals in LISA's frequency band, the joint EM and GW observation can be performed. Details of these VGBs in LISA's band can be found in [34, 35]. In LISA's SO1: When studying the formation and evolution of compact binary stars in the Milk Way Galaxy, the ability to detected and measure the (intrinsic and orbital) parameters of these VGBs is vital. Assuming a strain sensitivity without an effect from the SGWB, along with the estimation of the population of VGBs given in [39], LISA should be able to detect and resolve ~ 25000 VGBs.

We utilize data from VGBs obtained from Gaia DR3 [34]. Following the procedures outlined in [40], the characteristic strain of the GW signal emanating from VGBs, as illustrated in Fig. 1, is described by

$$h_c = \sqrt{T_{\rm obs}}\frac{2(G\mathcal{M})^{5/3}}{c^4 d}\pi^{2/3} f^{7/6}. \tag{7}$$

Here, $\mathcal{M}$ represents the chirp mass of each individual VGB, d signifies the distance to the source, and f corresponds to the GW frequency, which is twice the orbital frequency. For the sake of simplicity, the VGBs can be characterized as monochromatic GW signals with a set of parameters obtained from Gaia DR3. It is important to note that the SNR of VGBs can be readily calculated by taking the ratio of the characteristic strain h_c to the effective characteristic strain of the detector $S_{\rm eff}(f)$.

The EMRI is the inspiral of a stellar-mass compact object, such as a stellar-mass black hole, neutron star, or white drawf, into an SMBH. Here, we adopt the numerical kludge method [33, 41] to calculate the time-domain waveform of EMRIs. Because the inspiral signal of EMRIs can remain in LISA's frequency band for months to many years, and the binary might spend up to 10^5 or more orbits near the innermost stable circular orbit (ISCO), the events of the EMRI can provide accurate information on the space-time around the SMBH. This information can provide accurate measurements of the mass and spin of the SMBH and allow us to test Kerr geometry at a new high level. In SO3, the dynamics of dense nuclear clusters are probed using EMRIs, and in SO5, the fundamental nature of gravity and black holes is explored; therefore, the detection of EMRIs in the LISA frequency band can open a new channel of astrophysics discovery. Meanwhile, in SO6, the rate of expansion of the Universe is probed, and LISA will probe the topics in cosmology via EMRIs.

Because of the large uncertainty in the astrophysics of EMRIs, the LISA sensitivity without effects from the SGWB would result in a minimum rate of one case per year according to conservative EMRI population models [42]. For convenience of presentation, we only take one example of EMRI in Fig. 1.

According to the SNR shift caused by the presence of the SGWB within LISA noise, as depicted in Fig. 3, it is

evident that the SNRs of VGBs subjected to unabated $S_{\rm eff}(f)$ will experience a dramatic reduction. In fact, some of them drop below the threshold level of SNR = 8, rendering them undetectable by LISA. However, the detection of an SGWB originating from SMBHBs with SNR $\geq$ 100 holds the potential to significantly alleviate these SNR shifts for the majority of obscured VGBs, as illustrated in Fig. 3.

VI. CONCLUSION AND DISCUSSION

In light of recent discoveries from pulsar timing arrays, we now have compelling evidence of the SGWB produced by SMBHBs for the first time. In this context, we discuss the impacts of the SGWB from SMBHBs on the detection of compact binaries at LISA. It is worth noting that our arguments also apply to other spaceborne GW detectors, such as Taiji [43] and Tianqin [44]. Given that the SGWB from SMBHBs will introduce additional noise, denoted as $S_{\rm GW}(f)$, to LISA's strain sensitivity, it will shift the SNR of MBHBs, EMRIs, and VGBs with specific intrinsic and orbital parameters. This influence has the potential to impact the success of the LISA mission.

Based on our analysis, the effective sensitivity will obscure the GW signals of some VGBs and EMRIs, as directly shown in Fig. 1, leading to a reduction in their SNRs, as depicted in Fig. 3. Furthermore, the detectable redshift under specific SNR conditions for MBHBs will also decrease, as shown in Fig. 2. However, if we can resolve and eliminate GW signals from SMBHBs with an SNR above a certain threshold, all these influences can be effectively mitigated.

Therefore, the impacts on the detection of compact binaries due to the SGWB generated by SMBHBs are more significant than those of the expected galactic background. Understanding the SGWB and investigating its impact on the LISA mission are crucial for the success of space-borne GW detectors. Additionally, our results may offer an alternative perspective for the design of future GW detectors.

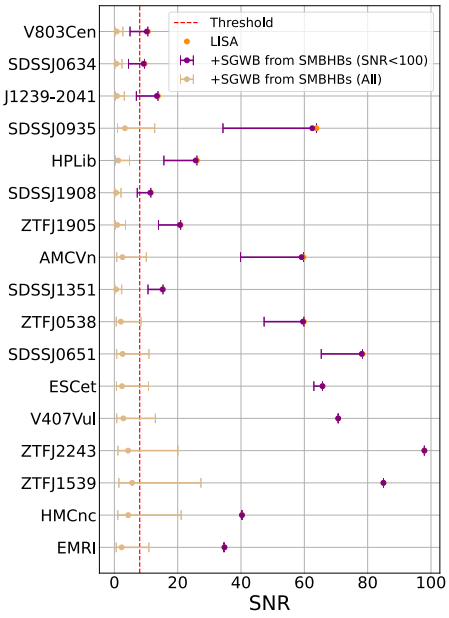

Fig. 3. (color online) SNR for VGB systems and an EMRI example. The threshold corresponds to an SNR of 8, signifying the minimum requirement for detecting these compact binary signals. The orange dots represent the SNR for LISA at its original sensitivity level, whereas the burlywood error bars illustrate the SNR for LISA sensitivity influenced by the SGWB generated by all SMBHBs. The purple error bar points indicate the SNR for LISA's sensitivity affected by the SGWB from SMBHBs with SNR values <100. For detailed information regarding the names and parameters of VGBs, refer to [34, 35], and for the parameters of the illustrative EMRI signal, refer to Fig. 1.

ACKNOWLEDGEMENTS

We would like to thank Xilong Fan and Lijin Shao for useful conversations. This study makes use of the Black Hole Perturbation Toolkit. We acknowledge the use of the HPC Cluster of ITP-CAS.

References

[1] M. Armano *et al.*, Phys. Rev. Lett. **116**, 231101 (2016)
[2] P. Amaro-Seoane *et al.* (LISA), *Laser Interferometer Space Antenna*, (2017), arXiv: 1702.00786[astroph.IM]
[3] P. Amaro Seoane *et al.* (LISA), Living Rev. Rel. **26**, 2 (2023), arXiv:2203.06016[gr-qc]
[4] L. Barack and C. Cutler, Phys. Rev. D **70**, 122002 (2004), arXiv:gr-qc/0409010
[5] T. Robson, Neil J. Cornish, and Chang Liu, Class. Quant. Grav. **36**, 105011 (2019), arXiv:1803.01944[astroph.HE]
[6] N. Cornish and T. Robson, J. Phys. Conf. Ser. **840**, 012024 (2017), arXiv:1703.09858[astro-ph.IM]
[7] Z. C. Chen, F. Huang, and Q. G. Huang, Astrophys. J. **871**, 97 (2019), arXiv:1809.10360[gr-qc]
[8] G. Agazie *et al.* (NANOGrav), Astrophys. J. Lett. **951**, L8 (2023), arXiv:2306.16213[astro-ph.HE]
[9] G. Agazie *et al.* (NANOGrav), Astrophys. J. Lett. **951**, L9 (2023), arXiv:2306.16217[astro-ph.HE]
[10] A. Afzal *et al.* (NANOGrav), Astrophys. J. Lett. **951**, L11 (2023), arXiv:2306.16219[astroph.HE]
[11] J. Antoniadis *et al.* (EPTA, InPTA:), Astron. Astrophys. **678**, A50 (2023), arXiv:2306.16214[astro-ph.HE]
[12] J. Antoniadis *et al.* (EPTA), Astron. Astrophys. **678**, A48 (2023), arXiv:2306.16224[astro-ph.HE]
[13] D. J. Reardon *et al.*, Astrophys. J. Lett. **951**, L6 (2023), arXiv:2306.16215[astro-ph.HE]

[14] A. Zic *et al*., *The Parkes Pulsar Timing Array Third Data Release*, (2023), arXiv: 2306.16230[astroph.HE]

[15] R. D. Nan, D. Li, C. J. Jin *et al*., Int. J. Mod. Phys. D **20**, 989 (2011), arXiv:1105.3794[astro-ph.IM]

[16] H. Xu *et al*., Res. Astron. Astrophys. **23**, 075024 (2023), arXiv:2306.16216[astro-ph.HE]

[17] G. Agazie *et al*. (NANOGrav), Astrophys. J. Lett. **952**, L37 (2023), arXiv:2306.16220[astro-ph.HE]

[18] J. Antoniadis *et al*. (EPTA), *The second data release from the European Pulsar Timing Array: V. Implications for massive black holes, dark matter and the early Universe*, (2023), arXiv: 2306.16227[astro-ph.CO]

[19] Y. C. Bi, Y. M. Wu, Z. C. Chen *et al*., Sci. China Phys. Mech. Astron. **66**, 120402 (2023), arXiv:2307.00722[astro-ph.CO]

[20] J. Ellis, M. Fairbairn, G. Franciolini *et al*., *What is the source of the PTA GW signal*? (2023), arXiv: 2308.08546[astro-ph.CO]

[21] Z. C. Li, Z. Jiang, X. L. Fan *et al*., Mon. Not. Roy. Astron. Soc. **527**, 3 (2024), arXiv:2304.08333[gr-qc]

[22] S. Y. Chen, Alberto Sesana, and Christopher J. Conselice, Mon. Not. Roy. Astron. Soc. **488**, 401 (2019), arXiv:1810.04184[astro-ph.GA]

[23] P. Ajith *et al*., Phys. Rev. D **77**, 104017 (2008), arXiv:0710.2335[gr-qc]

[24] X. J. Zhu, E. Howell, T. Regimbau *et al*., Astrophys. J. **739**, 86 (2011), arXiv:1104.3565[gr-qc]

[25] E. S. Phinney, *A Practical theorem on gravitational wave backgrounds*, (2001), arXiv: astro-ph/0108028

[26] N. Aghanim *et al*. (Planck), Astron. Astrophys. **641**, A6 (2020) [Erratum: Astron. Astrophys. **652**, C4 (2021)], arXiv: 1807.06209[astro-ph.CO]

[27] J. Kormendy and L. C. Ho, Ann. Rev. Astron. Astrophys. **51**, 511 (2013), arXiv:1304.7762[astro-ph.CO]

[28] C. Pitte, Q. Baghi, S. Marsat *et al*., Phys. Rev. D **108**, 044053 (2023), arXiv:2304.03142[gr-qc]

[29] S. Babak *et al*. (Mock LISA Data Challenge Task Force), Class. Quant. Grav. **27**, 084009 (2010), arXiv:0912.0548[gr-qc]

[30] S. Sachdev, T. Regimbau, and B. S. Sathyaprakash, Phys. Rev. D **102**, 024051 (2020), arXiv:2002.05365[gr-qc]

[31] B. Zhou, L. Reali, E. Berti *et al*. *Compact Binary Foreground Subtraction in Next-Generation Ground-Based Observatories*, (2022), arXiv: 2209.01221[gr-qc]

[32] D. S. Bellie, S. Banagiri, Z. Doctor *et al*., *The unresolved stochastic background from compact binary mergers detectable by nextgeneration ground-based gravitational-wave observatories*, (2023), arXiv: 2310.02517[gr-qc]

[33] A. J. K. Chua, C. J. Moore, and J. R. Gair, Phys. Rev. D **96**, 044005 (2017), arXiv:1705.04259[gr-qc]

[34] T. Kupfer *et al*., *LISA Galactic binaries with astrometry from Gaia DR3*, (2023), arXiv: 2302.12719[astro-ph.SR]

[35] T. Kupfer *et al*., *Lisa verification binaries*, (2023)

[36] M. Volonteri, Astron. Astrophys. Rev. **18**, 279 (2010), arXiv:1003.4404[astro-ph.CO]

[37] A. Sesana, F. Haardt, P. Madau *et al*., Astrophys. J. **611**, 623 (2004), arXiv:astro-ph/0401543

[38] A. Klein *et al*., Phys. Rev. D **93**, 024003 (2016), arXiv:1511.05581[grqc]

[39] S. Toonen, G. Nelemans, and S. P. Zwart, Astron. Astrophys. **546**, A70 (2012), arXiv:1208.6446[astro-ph.HE]

[40] T. Kupfer, V. Korol, S. Shah *et al*., Mon. Not. Roy. Astron. Soc. **480**, 302 (2018), arXiv:1805.00482[astro-ph.SR]

[41] S. Babak, H. Fang, J. R. Gair *et al*., Phys. Rev. D **75**, 024005 (2007), arXiv:gr-qc/0607007

[42] P. Amaro-Seoane, J. R. Gair, M. Freitag *et al*., Class. Quant. Grav. **24**, R113 (2007), arXiv:astro-ph/0703495

[43] Z. Luo, Y. Wang, Y. L. Wu *et al*., *The Taiji program: A concise overview*, Progress of Theoretical and Experimental Physics **2021**(5), 05A108 (2020)

[44] J. Luo *et al*. (TianQin), Class. Quant. Grav. **33**, 035010 (2016), arXiv:1512.02076[astro-ph.IM]